

Polyelliptic coordinates for solving the Schrödinger and Helmholtz equations

G. V. Kovalev ¹⁾

North Saint Paul, MN 55109, USA

Submitted 19 February 2013
Resubmitted

Several local elliptic coordinates are used to build a new polyelliptic coordinate system which is orthogonal and admits the separation of variables. Such coordinate systems can give the exact solutions of some unsolved problems in quantum mechanics and diffraction theory.

PACS: 03.65.Ge; 03.65.Fd; 03.65.Db; 02.30.Em

I. Introduction. The most powerful method for solving problems of quantum mechanics, diffraction theory and mathematical physics, in general, is the method of separation of variables. More than 60 years ago Robertson and Eisenhart [1, 2, 3] have shown that only 11 different coordinate systems allow the separation of the Schrödinger (SE) or Helmholtz (HE) equations in 3D space. The ellipsoidal system is the most general, the remaining 10 are the special cases of ellipsoidal. In particular, 3D Cartesian coordinates can be obtained from ellipsoidal when $\{f_1, f_2\} \rightarrow \infty$ (f is semi-focal distance) and the traditional spherical coordinates are received when $\{f_1, f_2\} \rightarrow 0$. The theory of separation of variables is well developed [4, 5] and has many advances since the time of publications of [1], but the ellipsoidal coordinates are still intriguing and many properties of ellipsoidal wave functions are unknown [6, 7, 8].

The purpose of this work is to show that the conclusion of Robertson and Eisenhart [1] is restricted to a single ellipsoidal coordinate system. But if we use several local ellipsoidal coordinate systems and combine them together by special rules described below, we can get a very large number of coordinate systems which are orthogonal and admit the separation of variables. In fact, even in 2D space the number of new coordinate systems is infinite because each new system is related to one specific convex polygon (or cone, polyhedron, finite cylinder, etc. for 3D case). The 3 examples for 2D space are built here and the separated ordinary differential equations for HE in new 2D coordinate system are derived in general form. On the reason which is clear from the context, these coordinates systems can be called 'polyelliptic' for 2D and 'polyellipsoidal', 'polyspheoidal', etc. for 3D spaces.

To illustrate the construction method, we consider 2D case where only 4 orthogonal coordinate system having the exact solutions of HE are known [4] and where elliptic coordinates, Fig.1(a), are the most general. The higher dimensional cases can be constructed using the similar rules and ideas. To build the new coordinates, we take three or more local elliptic coordinates with semi-focal distances f_1, f_2, f_3, \dots and put them on one plane letting the pair of focal points coincide in such a way that the interfocal line segments, denoted as L_{ij} : $L_{12} = 2f_1, L_{23} = 2f_2, \dots$, constitute an arbitrary convex polygon (see, e.g., triangle in Fig. 1(b)). Then we can observe the following properties of such construction:

- On the dashed lines N_{ij} in Fig.1(b), 2(a), 3, 4 (N is the numeric label of the vertex, $\{i, j\}$ are indices of a side of the polygon) the coordinate lines of 2 elliptic systems, i.e. ellipses and semi-hyperbolas, have the same tangent direction. Therefore, the coordinate lines at crossing the dashed lines preserve their directions and can be switched from one coordinate system to another. ²⁾
- The dashed lines and sides of n -polygon separate the XY-plane into $2n$ regions: $\Omega_{12}, \bar{\Omega}_{12}, \Omega_{31}, \bar{\Omega}_{31}, \dots$. Each region has a local elliptic coordinate system generated by one interfocal line, e.g. the region Ω_{12} is generated by L_{12} , the region $\bar{\Omega}_{23}$ generated by left side of L_{23} ³⁾, etc..

²⁾The short proof of this statement is in Fig.1(b), detailed proof will be published elsewhere.

³⁾We also introduce the 'polarization' of a focal line segment L_{ij} ; the positive direction is from focus f to negative focus $-f$ and on the right side of L_{ij} the local elliptic coordinate μ_i has the range $0 \leq \theta_i \leq \pi$, on the left side the range is $\pi \leq \theta_i \leq 2\pi$. For short, the left side is denoted by bar always. In such conventions, the positive path around a convex polygon is the counterclockwise, Fig. 1(a), and region $\bar{\Omega}_{23}$ is generated by left side of the interfocal line L_{23} .

¹⁾e-mail: kovalevgennady@qwest.net

- The coordinate lines of new common system are smooth everywhere outside the perimeter of the polygon and it is possible to introduce a common 'polyelliptic' coordinates μ_c, θ_c for this region including the perimeter.
- All congruent polygons have the similar type of 'polyelliptic' coordinate system. The HE and SE with potential function having Stäckel form for these system gives a new type of orthogonal eigenfunctions and eigenvalues similar to Mathieu's types. Noncongruent polygons give the different 'polyelliptic' coordinates and different types of orthogonal eigenfunctions and eigenvalues.
- There is a 'protected area' Ω_0 (interior of the convex polygon), which is not covered by this method. However, in many cases the Ω_0 can be covered by another orthogonal coordinates (e.g., Cartesian, as in Fig.7). In some cases (diffraction, QM), this coverage is not necessary because the sides of polygon can satisfy Dirichlet's conditions.
- When one semifocal distance $f_i \rightarrow 0$, the 'polyelliptic' coordinates generated by n-polygon is topologically transformed to another 'polyelliptic' system generated by (n-1)-polygon. In particular, when $f_3 \rightarrow 0$ the triangular 'polyelliptic' coordinates are transformed to an ordinary elliptic coordinate system. Hence, a single elliptic coordinate system Fig.1(a) is a particular case of the general 'polyelliptic' coordinates Fig.3(a).

II. Triangle Elliptic Coordinates and other. The local elliptic coordinate system (μ_i, θ_i) in region Ω_{ij} or $\bar{\Omega}_{ij}$ for arbitrary orientation and displacement of the focal line L_{ij} is defined as

$$\begin{aligned} x &= A_i \cos \beta_{ij} - B_i \sin \beta_{ij} + \frac{x_i + x_j}{2}, \\ y &= A_i \sin \beta_{ij} + B_i \cos \beta_{ij} + \frac{y_i + y_j}{2}, \end{aligned} \quad (1)$$

where A_i, B_i are usual elliptic transformation functions:

$$A_i = f_i \cosh \mu_i \cos \theta_i, \quad B_i = f_i \sinh \mu_i \sin \theta_i, \quad (2)$$

and β_{ij} is the angle between negative direction of focal distance L_{ij} and positive direction of axis x , Fig. 1(b). When two points (x', y') , (x'', y'') coincide on the dashed semi-infinite line, the relations between two major elliptic semi-axes: $ae = (r_a + r_b)/2$, $\bar{ae} = (\bar{r}_a + \bar{r}_b)/2$, and two major hyperbolic semi-axes: $ah = (r_a - r_b)/2$, $\bar{ah} = (\bar{r}_a - \bar{r}_b)/2$, are $\bar{ae} - ae = f$ and $\bar{ah} + ah = \pm f$. These relations in triangle 'polyelliptic' coordinates for all major elliptic and hyperbolic semi-axes are (1-st column denotes the dashed lines in Fig. 3(a)):

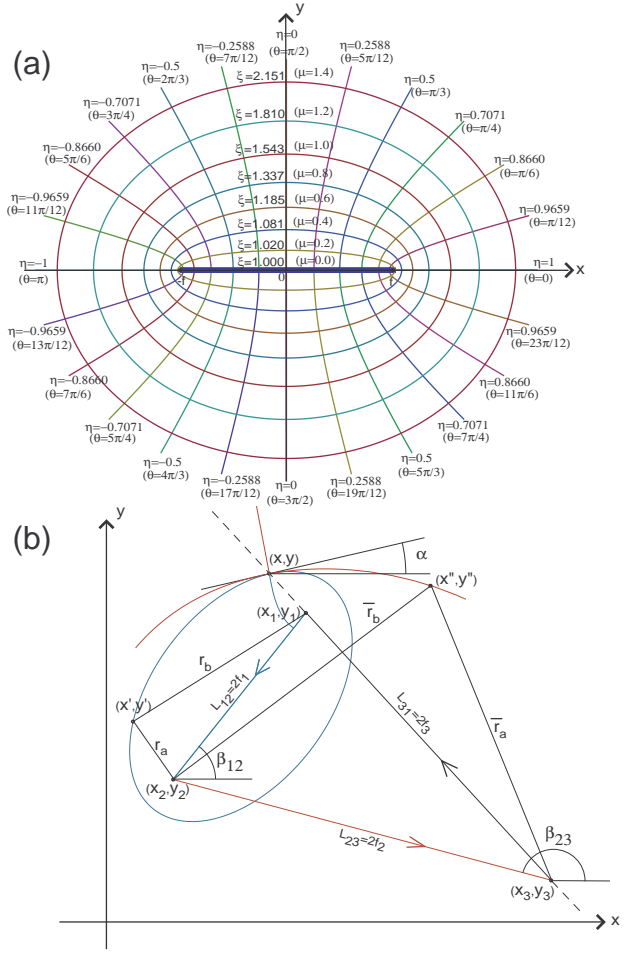


Fig.1. (a) The elliptic coordinates ξ, η : $x = f\xi\eta$, $y = f\sqrt{(\xi^2 - 1)(1 - \eta^2)}$. Upper and lower semi-hyperbolas are different coordinate lines, therefore instead ξ, η one should use μ, θ : $\xi = \cosh \mu$, $\eta = \cos \theta$. (b) Two elliptic coordinate systems with focal distances L_{12}, L_{23} and common focal point (x_2, y_2) have the same tangent derivative $(\frac{dy(x)}{dx})_{12} = (\frac{dy(x)}{dx})_{23} = \tan \alpha$ to their ellipses (blue for L_{12} and red for L_{23}) on dashed straight line coming out from the point (x_1, y_1) . The same is true for semi-hyperbolas.

$$\begin{aligned} 1_{31} : \quad & \bar{ae}_2 - ae_1 = f_3, \quad \bar{ah}1_{31} + ah1_{31} = f_3; \\ 2_{23} : \quad & \bar{ae}_3 - ae_1 = f_2, \quad \bar{ah}2_{23} + ah2_{23} = -f_2; \\ 2_{12} : \quad & \bar{ae}_3 - ae_2 = f_1, \quad \bar{ah}2_{12} + ah2_{12} = f_1; \\ 3_{31} : \quad & \bar{ae}_1 - ae_2 = f_3, \quad \bar{ah}3_{31} + ah3_{31} = -f_3; \\ 3_{23} : \quad & \bar{ae}_1 - ae_3 = f_2, \quad \bar{ah}3_{23} + ah3_{23} = f_2; \\ 1_{12} : \quad & \bar{ae}_2 - ae_3 = f_1, \quad \bar{ah}1_{12} + ah1_{12} = -f_1. \end{aligned} \quad (3)$$

The similar relations hold for any polyelliptic system generated by a convex n-polygon and allow to introduce the common elliptic coordinates. Indeed, all major ellip-

tic semi-axes (3) in all regions can be expressed through just one, say \overline{ae}_2 :

$$\begin{aligned} ae_1 &= \overline{ae}_2 - f_3, & \overline{ae}_3 &= \overline{ae}_2 - f_3 + f_2, \\ ae_2 &= \overline{ae}_2 - f_3 + f_2 - f_1, & \overline{ae}_1 &= \overline{ae}_2 + f_2 - f_1, \\ ae_3 &= \overline{ae}_2 - f_1, \end{aligned} \quad (4)$$

so the value \overline{ae}_2 can be considered as a common 'radial' coordinate ae_c . We note, however, that the range of $ae_c = \overline{ae}_2$ is from $f_1 + f_3$ to ∞ and all others ae 's are positive. From ae_c , we can deduce another 'radial' common coordinate μ_c with 'universal' range:

$$\mu_c = \operatorname{arccosh}\left[\frac{ae_c}{f_1 + f_3}\right], \quad 0 \leq \mu_c \leq \infty. \quad (5)$$

We can take any other elliptic semi-axes ae as a common 'radial' coordinate using (3). The respective transition from ae to μ_c will give the similar 'radial' common coordinate μ_c with the same range $0 \leq \mu_c \leq \infty$.

The angular common coordinate θ_c is also defined from (3), but its definition is more complicated. For our triangle, the hyperbolas lying in the ranges of local major hyperbolic semi-axes,

$$\begin{aligned} -\cos \gamma_2 \leq \frac{ah_1}{f_1} \leq \cos \gamma_1, & \quad -\cos \gamma_3 \leq \frac{ah_2}{f_2} \leq \cos \gamma_2, \\ -\cos \gamma_1 \leq \frac{ah_3}{f_3} \leq \cos \gamma_3, \end{aligned} \quad (6)$$

remains the same and incorporated in common coordinate system directly, see Fig. 2(b). Other angular coordinate lines are built from 2 pieces of hyperbolas which are smoothly connected to each other on the dashed lines. For this we use additional relations $ah = F(ae)$, e.g.

$$\begin{aligned} ah_{131} &= f_1 \frac{ae_1 \cos \gamma_1 + f_1}{ae_1 + f_1 \cos \gamma_1}, & ah_{231} &= -f_1 \frac{ae_1 \cos \gamma_2 + f_1}{ae_1 + f_1 \cos \gamma_2}, \\ \overline{ah}_{331} &= -f_1 \frac{\overline{ae}_1 \cos \gamma_1 - f_1}{\overline{ae}_1 - f_1 \cos \gamma_1}, & \overline{ah}_{323} &= f_1 \frac{\overline{ae}_1 \cos \gamma_2 - f_1}{\overline{ae}_1 - f_1 \cos \gamma_2}, \end{aligned} \quad (7)$$

which are the equations of dashed straight lines in the local elliptic coordinates generated by L_{12} . There are 3 local coordinates, so we have 12 equations for our triangle polyelliptic system (other 8 equations are not shown in (7), but can be written by analogy). The local angular coordinates θ_{131} generated by L_{12} and $\overline{\theta}_{131}$ generated by left side of L_{23} are related (see 1st eq. in 3rd column of (3)) by the equation on boundary line l_{31} , Fig.1(b), Fig. 2(a)

$$\overline{\theta}_{131} = \arccos\left[\frac{f_3 - f_1 \cos \theta_{131}}{f_2}\right], \quad 0 \leq \theta_{131} \leq \gamma_1. \quad (8)$$

If we assume that origin of θ_c is 0 when the local angular coordinate $\theta_{131} = 0$, then the common angular coordinate θ_c is

$$\theta_c = \theta_{v1} - \overline{\theta}_{131}, \quad 0 \leq \theta_c \leq \phi_1. \quad (9)$$

Here we introduce the angle θ_{v1} linked to the hyperbola coming through the vertex 1 of triangle (see Fig. 2(a)):

$$\theta_{v1} = \arccos\left[\frac{f_3 - f_1}{f_2}\right], \quad \phi_1 = \theta_{v1} - \gamma_3. \quad (10)$$

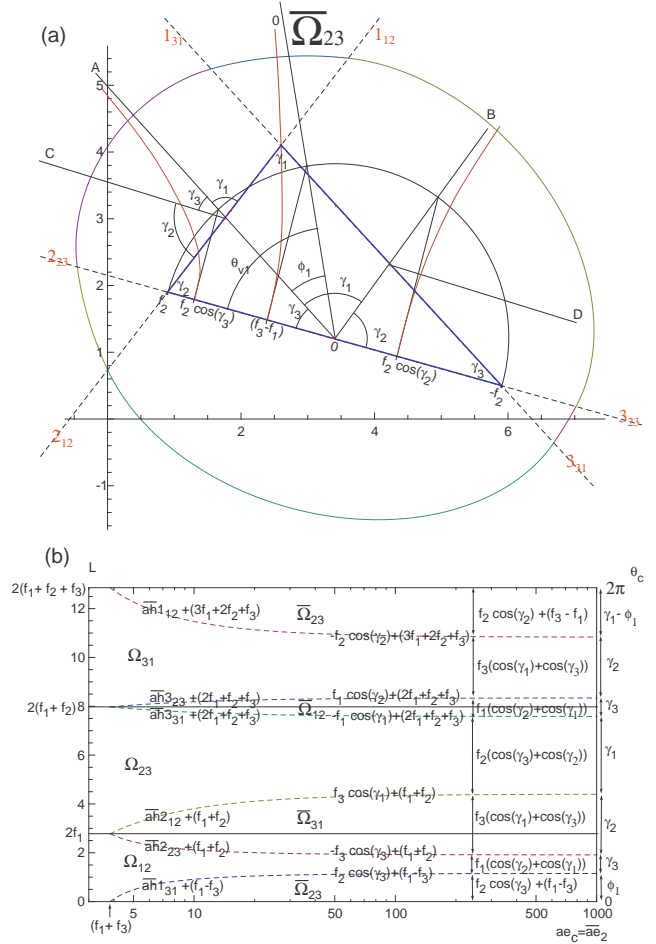


Fig.2. (a) The triangle 'polyelliptic' coordinates μ_c, θ_c are built from 3 local elliptic coordinates: $L_{12} = 2.78$, $L_{23} = 5.19$, $L_{31} = 4.88$; $\gamma_1 = 80.2^\circ$, $\gamma_2 = 67.95^\circ$, $\gamma_3 = 31.85^\circ$. (b) All horizontal straight lines present the hyperbolic or hyperbolic-like coordinates; the curved dashed lines present the the straight lines l_{31}, l_{23}, \dots

The range $0 \leq \theta_{131} \leq \gamma_1$ in (8) corresponds to the variation of the angle $\overline{\theta}_{131}$ inside the part of region $\overline{\Omega}_{23}$

$$\gamma_3 \leq \overline{\theta}_{131} \leq \theta_{v1}. \quad (11)$$

The range of $\overline{\theta}_{131}$ is always less than the range of θ_{131} (e.g., compare the data using Fig.2(a)). This compression reduces the apparent angular span generated by all sides of triangle from $3 \times 180^\circ = 540^\circ$ to the usual 360° ,

Fig. 2(a). The identification of the hyperbola-like coordinates can only be done using the hyperbolas lying in $\bar{\Omega}_{23}, \bar{\Omega}_{31}, \bar{\Omega}_{12}$ where they go to infinity. There is also a simple way to find the coordinate net θ_c using rectangular plot Fig. 2(b). The horizontal axis presents the ae_c (in logarithmic scale) and vertical axis presents the perimeter or the common angle θ_c . Going through the boundaries of 6 regions and 6 additional adjacent regions with hyperbola-like coordinates, we can receive the coefficients A_i, B_i in (1) for 12 regions (for short we use here the radial coordinate $ae_c = (f_1 + f_3) \cosh \mu_c$):

$$\begin{aligned} \bar{A}_2 &= ae_c \cos[\theta - \theta_{v1}], \quad \bar{B}_2 = \sqrt{(ae_c)^2 - f_2^2} \sin[\theta_c - \theta_{v1}]; \\ \bar{A}_{2F} &= (ae_c - f_3) \left(\frac{f_3 - f_2 \cos[\theta - \theta_{v1}]}{f_1} \right), \\ \bar{B}_{2F} &= \sqrt{((ae_c - f_3)^2 - f_1^2) \left(1 - \left(\frac{f_3 - f_2 \cos[\theta_c - \theta_{v1}]}{f_1} \right)^2 \right)}; \\ A_1 &= (ae_c - f_3) \cos[\theta_c - (\theta_{v1} - \gamma_3 - \gamma_1)], \\ B_1 &= \sqrt{(ae_c - f_3)^2 - f_1^2} \sin[\theta_c - (\theta_{v1} - \gamma_3 - \gamma_1)]; \\ \bar{A}_{3B} &= (ae_c - f_3) \left(\frac{-f_2 - f_3 \cos[\theta_{v1} + \gamma_1 + \gamma_2 - \theta_c]}{f_1} \right), \\ \bar{B}_{3B} &= \sqrt{(ae_c - f_3)^2 - f_1^2} \times \\ &\quad \sqrt{1 - \left(\frac{-f_2 - f_3 \cos[\theta_{v1} + \gamma_1 + \gamma_2 - \theta_c]}{f_1} \right)^2}; \\ \bar{A}_3 &= (ae_c - f_3 + f_2) (\cos[\theta_{v1} + \gamma_1 + \gamma_2 - \theta_c]), \\ \bar{B}_3 &= \sqrt{(ae_c - f_3 + f_2)^2 - f_2^2} \sin[\theta_{v1} + \gamma_1 + \gamma_2 - \theta_c]; \\ \bar{A}_{3F} &= (ae_c - f_3 + f_2 - f_1) \left(\frac{f_1 - f_3 \cos[\theta_{v1} + \gamma_1 + \gamma_2 - \theta_c]}{f_2} \right), \\ \bar{B}_{3F} &= \sqrt{(ae_c - f_3 + f_2 - f_1)^2 - f_2^2} \times \\ &\quad \sqrt{1 - \left(\frac{f_1 - f_3 \cos[\theta_{v1} + \gamma_1 + \gamma_2 - \theta_c]}{f_2} \right)^2}; \\ A_2 &= (ae_c - f_3 + f_2 - f_1) (\cos[\theta_c - \theta_{v1}]), \\ B_2 &= \sqrt{(ae_c - f_3 + f_2 - f_1)^2 - f_2^2} \sin[\theta_c - \theta_{v1}]; \\ \bar{A}_{1B} &= (ae_c - f_3 + f_2 - f_1) \frac{-f_3 - f_1 \cos[\theta_{v1} + \gamma_1 + 2\gamma_2 + \gamma_3 - \theta_c]}{f_2}, \\ \bar{B}_{1B} &= \sqrt{(ae_c - f_3 + f_2 - f_1)^2 - f_2^2} \times \\ &\quad \sqrt{1 - \left(\frac{-f_3 - f_1 \cos[\theta_{v1} + \gamma_1 + 2\gamma_2 + \gamma_3 - \theta_c]}{f_2} \right)^2}; \\ \bar{A}_1 &= (ae_c + f_2 - f_1) (\cos[\theta_{v1} + \gamma_1 + 2\gamma_2 + \gamma_3 - \theta_c]), \\ \bar{B}_1 &= \sqrt{(ae_c + f_2 - f_1)^2 - f_1^2} \times \\ &\quad \sin[\theta_{v1} + \gamma_1 + 2\gamma_2 + \gamma_3 - \theta_c]; \\ \bar{A}_{3F} &= (ae_c - f_1) \left(\frac{f_2 - f_1 \cos[\theta_{v1} + \gamma_1 + 2\gamma_2 + \gamma_3 - \theta_c]}{f_3} \right), \\ \bar{B}_{3F} &= \sqrt{(ae_c - f_1)^2 - f_3^2} \times \\ &\quad \sqrt{1 - \left(\frac{f_2 - f_1 \cos[\theta_{v1} + \gamma_1 + 2\gamma_2 + \gamma_3 - \theta_c]}{f_3} \right)^2}; \\ A_3 &= (ae_c - f_1) (\cos[\theta_c - (\theta_{v1} + \pi - \gamma_3)]), \\ B_3 &= \sqrt{(ae_c - f_1)^2 - f_3^2} \sin[\theta_c - (\theta_{v1} + \pi - \gamma_3)]; \\ \bar{A}_{2B} &= (ae_c - f_1) \left(\frac{-f_1 - f_2 \cos[\theta_{v1} + 2\pi - \theta_c]}{f_3} \right), \\ \bar{B}_{2B} &= \sqrt{(ae_c - f_1)^2 - f_3^2} \times \\ &\quad \sqrt{1 - \left(\frac{-f_1 - f_2 \cos[\theta_{v1} + 2\pi - \theta_c]}{f_3} \right)^2}. \end{aligned}$$

These long but rather simple expressions allow to build any polyelliptic coordinates outside the arbitrary triangle, Fig.3. If we are moving around counterclockwise, the coefficients with index “B” correspond to compressed region before of $\bar{\Omega}$, coefficients with index “F” correspond to compressed region in front of $\bar{\Omega}$. As example, the shaded area in Fig.3(a) includes 3 regions: with indices “B”, “F” and region $\bar{\Omega}_{31}$ itself. If we take degen-

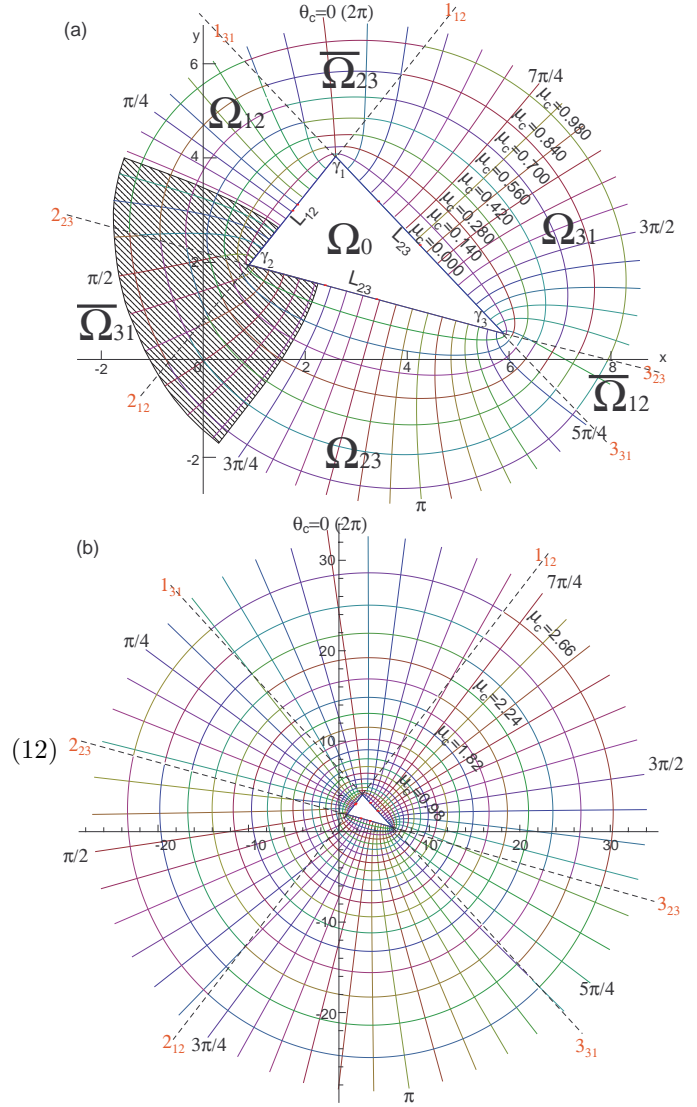


Fig.3 (a) The final structure of arbitrary triangle 'polyelliptic' coordinates μ_c, θ_c with: $L_{12} = 2.78, L_{23} = 5.19, L_{31} = 4.88; \gamma_1 = 80.2^\circ, \gamma_2 = 67.95^\circ, \gamma_3 = 31.85^\circ$. Shade at one corner shows the area of hyperbola-like coordinates. (b) The same coordinate system for large μ_c becomes similar to the polar coordinates.

erated triangle $f_1 = f_2, f_3 = 0$, the triangle polyelliptic system becomes the simple elliptic coordinates. Tak-

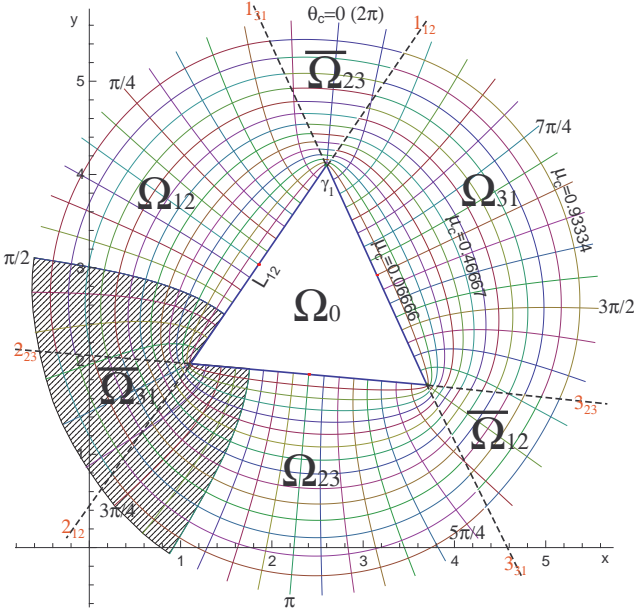


Fig.4. The equilateral triangle 'polyelliptic' coordinates μ_c, θ_c with $f_1 = f_2 = f_3 = 1.3$. Shade at one corner shows the area of hyperbola-like coordinates.

ing $f_1 = f_2 = f_3 = f$, we can produce the equilateral triangle polyelliptic system, Fig. 4. It is not difficult to modify the equations (12) and build also the square polyelliptic system, Fig.5. The interesting feature of the square and rectangular polyelliptic system is the absence of the regions with true hyperbolas. All angular coordinates (except 8 straight lines coming out from vertices and centers of interfocal lines) are built from two pieces of hyperbolas. The construction of n-polygon polyelliptic system may include the angular coordinates which are built from $n - 1$ pieces of hyperbolas.

II. Stäckel form and differential equations.

The HE $\Delta\Psi + k^2\Psi = 0$ in 2D Cartesian coordinates can be written in a general curvilinear orthogonal form

$$\frac{1}{H_1 H_2} \left[\partial_1 \left(\frac{H_2}{H_1} \partial_1 \Psi \right) + \partial_2 \left(\frac{H_1}{H_2} \partial_2 \Psi \right) \right] + k^2 \Psi = 0, \quad (13)$$

where $H_i = \sqrt{g_{i,i}}$ are scale factors, $\partial_i = \partial/\partial q_i$. We can show that the metric $g_{i,j}$ for polyelliptic coordinates θ_c, μ_c in the exterior of n-polygon are diagonal and $H_{\theta_c} = \sqrt{(\partial_{\theta_c} x)^2 + (\partial_{\theta_c} y)^2}$, $H_{\mu_c} = \sqrt{(\partial_{\mu_c} x)^2 + (\partial_{\mu_c} y)^2}$ are continuous functions of θ_c, μ_c having the Stäckel expression [9]

$$\begin{aligned} H_{\theta_c}^2 &= g_1(\theta_c)[h_1(\mu_c) + h_2(\theta_c)], \\ H_{\mu_c}^2 &= g_2(\mu_c)[h_1(\mu_c) + h_2(\theta_c)], \end{aligned} \quad (14)$$

where g_1, g_2, h_1, h_2 are continuous functions consisting of pieces from trigonometric or hyperbolic functions. It

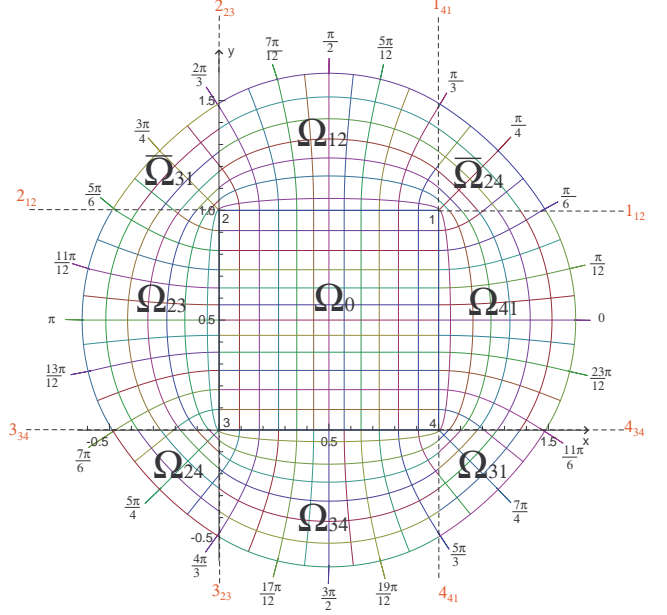


Fig.5. Square 'polyelliptic' coordinates μ_c, θ_c . The 'protected area' Ω_0 is covered by Cartesian coordinates with nonuniform scale in x - and y -directions.

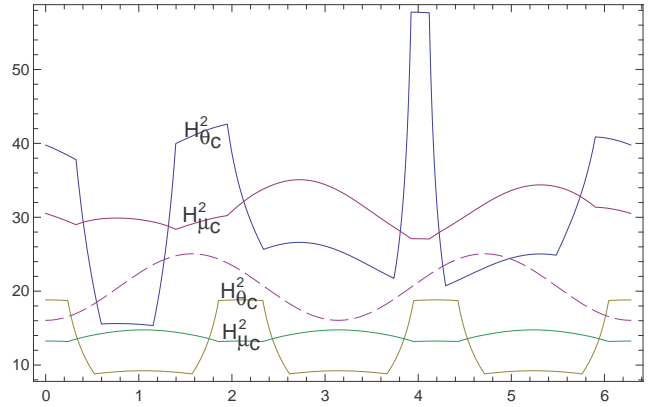


Fig.6. Scale factors: $H_{\theta_c}^2, H_{\mu_c}^2$ in triangle coordinates Fig.3 (blue, red), Fig.4 (yellow, green), calculated for fixed $\mu_c = 1.1$. Dashed curve presents Mathieu's elliptic scale factors for $f = 3, \mu = 1.1$.

is clear that derivatives of (14) will be piecewise continuous functions having a finite jumps on the boundaries of the regions. As exsample in the region $\bar{\Omega}_{23}$ (\bar{A}_2, \bar{B}_2 are taken from (12)) these scale factors are

$$H_{\theta_c}^2 = (f_1 + f_3)^2 \cosh[\mu_c]^2 - f_2^2 \cos[\theta_c - \theta_{v1}]^2, \quad (15)$$

$$H_{\mu_c}^2 = \frac{(f_1 + f_3)^2}{(f_1 + f_3)^2 \cosh[\mu]^2 - f_2^2} \times ((f_1 + f_3)^2 \cosh[\mu_c]^2 - f_2^2 \cos[\theta_c - \theta_{v1}]^2), \quad (16)$$

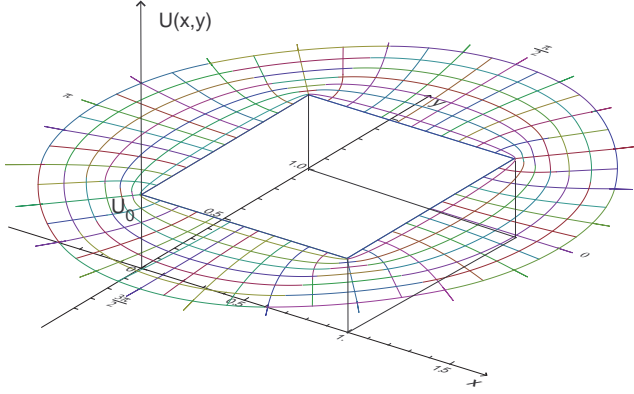


Fig.7. Square-well potential with square shape. In 'square-elliptic' coordinates the problem of finding the energy levels and wave eigenfunctions is solvable.

where $g_1(\theta_c) = 1$, and $g_2(\mu_c)$ is 1st term of (16). For short, we skip the similar expression for other regions. The Fig.6 illustrates these scale factors as a function of θ_c for arbitrary and equilateral triangle coordinates, Fig.4, as well as Mathieu's scale factors for comparison. Searching for solutions in the form $\Psi = \Psi_1(\theta_c)\Psi_2(\mu_c)$, the HE (14) can be split up into two ordinary differential equations with separation constant λ :

$$\partial_{\theta_c}^2 \Psi_1 - \frac{g_1'}{2g_1} \partial_{\theta_c} \Psi_1 + g_1[\lambda + k^2 h_2] \Psi_1 = 0, \quad (17)$$

$$\partial_{\mu_c}^2 \Psi_2 - \frac{g_2'}{2g_2} \partial_{\mu_c} \Psi_2 - g_2[\lambda - k^2 h_1] \Psi_2 = 0. \quad (18)$$

If the ODE (17) can be solved in the exterior of polygon with periodic condition $\Psi_1(0) = \Psi_1(2\pi)$, it gives a new set of eigenfunctions specific for this particular polygon with the corresponding eigenvalues. The equation (18) should give the radial solution for HE. Note that set ODE (17)-(18) becomes Mathieu's equations[3] when we use the elliptic scale factors $H_{\theta_c} = H_{\mu_c} = \sqrt{\cosh^2 \mu_c - \cos^2 \theta_c}$, where g_1, g_2 are constants.

III. Applications. There are many possible applications of polyelliptic coordinates, and we outline only several.

(a) The n-polygon polyelliptic system has a 'protected' area, which can be thought of as a infinite high potential. If a plane wave is expanded on eigenfunctions of ODE (17)-(18) with Dirichlet condition on perimeter of polygon, we should immediately receive exact solution for scattering problem in variety of applications which employ the sharp edges (acoustics, radar, etc.).

(b) The rotation of equilateral Fig.4 or isosceles triangle elliptic coordinates around axis of symmetry creates the new types of 3D polyelliptic coordinates which

are neither prolate or oblate. The 'protected' volume will be a cone and finding the eigenfunctions can give the solution for this important 3D scattering problem.

(c) SE for 2D potential, Fig. 7,

$$U(x, y) = \begin{cases} 0, & 0 \leq x \leq a, 0 \leq y \leq a; \\ U_0, & x < 0, x > a, y < 0, y > a, \end{cases} \quad (19)$$

as previously thought, does not have a separable system⁴⁾ because the square perimeter does not correspond to any coordinate line. However, it does correspond to $\mu_c = 0$ in square polyelliptic system Fig.5,7 and the surrounding of square has two independent wave functions Ψ_1, Ψ_2 which allow to solve the spectrum problem with potential (19) if eigenfunctions of (17)-(18) are found.

IV. Summary. We have presented an infinite family of new orthogonal coordinate systems which admit the separation of variables for SE and HE in 2D space and assume the existence of such system in 3D space. Each coordinate system is related to one particular polygon and has two ODE describing a set of eigenfunctions with corresponding eigenvalues. If the eigenfunctions outside the polygon can be calculated, this approach may help to solve some long standing problems.

1. H. P. Robertson, Math. Ann. **98**, 749 (1928); L. P. Eisenhart, Ann. Math. **35**, 284, (1934); Phys. Rev. **45**, 427 (1934); **74**, 87 (1948).
2. P. Moon and D.E. Spencer, Field Theory Handbook, Springer-Verlag, Berlin, 1988.
3. P.M. Morse and H. Feshbach, Methods of Theoretical Physics, vol.1-2, McGraw-Hill Book Co., New York, 1953.
4. W. Miller, Jr. Symmetry and separation of variable, Addison Wesley, 1977.
5. E. G. Kalnins, Separation of Variables for Riemannian Spaces of Constant Curvature, Longman Scientific and Technical, Essex, 1986.
6. M. V. Fedoryuk, Math. Notes **46**, 804-811 (1989).
7. V. Rokhlin and Hong Xiao, Appl. Comput. Harmon. Anal. **22**, 105-123 (2007).
8. D. Slepian, SIAMReview, **25**, Issue 3, 379-393 (1983).
9. P. Stackel, Mathematische Annalen, **35**, 91-103 (1890).
10. S.D. Poisson, "Memoire sur l'equilibre et le mouvement des corps elastiques" in "Memoires de l'Institut", v.VIII Paris, 1828.
11. J.E. Goell, Bell. Syst. Tech. J., **48**, 2133 (1969).
12. E.A.J. Marcatili, Bell. Syst. Tech. J., **48**, 2071 (1969).

⁴⁾HE for 2D box with infinite high potential wall was solved by Poisson [10]. The problem of scattering on square box (finite of infinite) and spectral problem for potential (19) have not been exactly solved yet. But due to importance of this problem in fiber optics, there are several numerical solutions[11],[12]